UC San Diego
UC San Diego Previously Published Works

Title

Evolution of DNA Methylation Is Linked to Genetic Aberrations in Chronic Lymphocytic Leukemia

Permalink

https://escholarship.org/uc/item/3s48x9hz

Journal

Cancer Discovery, 4(3)

ISSN

2159-8274

Authors

Oakes, Christopher C
Claus, Rainer
Gu, Lei
et al.

Publication Date

2014-03-01

DOI

10.1158/2159-8290.cd-13-0349

Peer reviewed

Evolution of DNA Methylation Is Linked to Genetic Aberrations in Chronic Lymphocytic Leukemia

Christopher C. Oakes[1,7], **Rainer Claus**[1,7], **Lei Gu**[1,2], **Yassen Assenov**[1], **Jennifer Hüllein**[5], **Manuela Zucknick**[3], **Matthias Bieg**[2], **David Brocks**[1], **Olga Bogatyrova**[1], **Christopher R. Schmidt**[1], **Laura Rassenti**[10], **Thomas J. Kipps**[10], **Daniel Mertens**[4,8], **Peter Lichter**[4,9], **Hartmut Döhner**[8], **Stephan Stilgenbauer**[8], **John C. Byrd**[11], **Thorsten Zenz**[5,6], and **Christoph Plass**[1,9]

[1]Division of Epigenomics and Cancer Risk Factors, National Center for Tumor Diseases (NCT), The German Cancer Research Center (DKFZ)

[2]Division of Theoretical Bioinformatics, National Center for Tumor Diseases (NCT), The German Cancer Research Center (DKFZ)

[3]Division of Biostatistics, National Center for Tumor Diseases (NCT), The German Cancer Research Center (DKFZ)

[4]Division of Molecular Genetics, National Center for Tumor Diseases (NCT), The German Cancer Research Center (DKFZ)

[5]Department of Translational Oncology, National Center for Tumor Diseases (NCT), The German Cancer Research Center (DKFZ)

[6]Department of Medicine V, University of Heidelberg, Heidelberg

[7]Department of Medicine, University of Freiburg Medical Center, Freiburg

[8]Department of Internal Medicine III, University of Ulm, Ulm

[9]The German Cancer Consortium, Germany

Corresponding Author: Christoph Plass, Division of Epigenomics and Cancer Risk Factors, The German Cancer Research Center (DKFZ), Im Neuenheimer Feld 280, 69120 Heidelberg, Germany. Phone: 49-6221-423330; Fax: 49-6221-423359; c.plass@dkfz.de.

Disclosure of Potential Conflicts of Interest
T. Zenz has received a commercial research grant from Roche Molecular Systems. No potential conflicts of interest were disclosed by the other authors.

Authors' Contributions
Conception and design: C.C. Oakes, R. Claus, L. Gu, P. Lichter, S. Stilgenbauer, J.C. Byrd, C. Plass
Development of methodology: C.C. Oakes, R. Claus, L. Gu, J.C. Byrd
Acquisition of data (provided animals, acquired and managed patients, provided facilities, etc.): C.C. Oakes, R. Claus, J. Hüllein, L. Rassenti, T.J. Kipps, H. Döhner, S. Stilgenbauer, J.C. Byrd, T. Zenz
Analysis and interpretation of data (e.g., statistical analysis, biostatistics, computational analysis): C.C. Oakes, R. Claus, L. Gu, Y. Assenov, J. Hüllein, M. Zucknick, M. Bieg, D. Brocks, O. Bogatyrova, C.R. Schmidt, P. Lichter, S. Stilgenbauer, T. Zenz
Writing, review, and/or revision of the manuscript: C.C. Oakes, L. Gu, J. Hüllein, M. Zucknick, L. Rassenti, D. Mertens, H. Döhner, S. Stilgenbauer, J.C. Byrd, T. Zenz, C. Plass
Administrative, technical, or material support (i.e., reporting or organizing data, constructing databases): L. Gu, J. Hüllein, M. Bieg, L. Rassenti, J.C. Byrd
Study supervision: C. Plass

¹⁰Department of Medicine, University of California at San Diego Moores Cancer Center, La Jolla, California

¹¹Division of Hematology, The Ohio State University, Columbus, Ohio

Abstract

Although clonal selection by genetic driver aberrations in cancer is well documented, the ability of epigenetic alterations to promote tumor evolution is undefined. We used 450k arrays and next-generation sequencing to evaluate intratumor heterogeneity and evolution of DNA methylation and genetic aberrations in chronic lymphocytic leukemia (CLL). CLL cases exhibit vast interpatient differences in intratumor methylation heterogeneity, with genetically clonal cases maintaining low methylation heterogeneity and up to 10% of total CpGs in a monoallelically methylated state. Increasing methylation heterogeneity correlates with advanced genetic subclonal complexity. Selection of novel DNA methylation patterns is observed only in cases that undergo genetic evolution, and independent genetic evolution is uncommon and is restricted to low-risk alterations. These results reveal that although evolution of DNA methylation occurs in high-risk, clinically progressive cases, positive selection of novel methylation patterns entails coevolution of genetic alteration(s) in CLL.

INTRODUCTION

The impact of genetic events on the development and progression of cancer has been clearly demonstrated through the use of murine genetic tumor models and through the association of recurrent mutations and genomic aberrations with clinical outcome. Epigenetic differences are vast between tumor and perceived normal tissues, as well as between patients, typically involving thousands of loci in a particular genome (1). Epigenetic patterns between various normal cell types are highly divergent, and are key in determining cell phenotypes and function (2, 3). Although several oncogenes and tumor-suppressor genes are found to have recurrently altered epigenetic states in tumors, which contribute to the cancer cell phenotype, a direct, causative role for the bulk of epigenetic alterations is unclear. Recent tumor genome–sequencing efforts have uncovered mutations affecting numerous genes with known epigenetic functions in cancer (reviewed in ref. 4), which further support an important role for epigenetics in cancer development.

Evolution and resulting genetic tumor heterogeneity are currently under investigation for many malignancies, as they may explain acquired resistance to therapies. Pronounced intratumor genetic variation has been recently appreciated for solid tumors (5–7), acute leukemias (8, 9), and chronic lymphocytic leukemia (CLL; refs. 10, 11). In comparison with other cancers, CLL offers several advantages to study epigenetic heterogeneity and evolution of tumor cell populations. First, CLL is a malignancy that possesses a mature, differentiated cellular phenotype that is epigenetically stable throughout the disease course, even following treatment (12). CLL tumor samples can be obtained at near-complete purity, and allow for the assignment of tumor subpopulations to the original founder cell via the unique rearrangement of the B-cell receptor. Finally, the epigenetic patterns in CLL are consistent between peripheral blood and lymph node compartments (12), allowing for the

overall tumor cell population to be represented upon sampling. Furthermore, evolution of genetic alterations in CLL is found to occur in patients with poor prognostic markers and to be associated with inferior outcome (13).

Epigenetic alterations, such as DNA methylation, have the potential to add complexity to the tumor cell population. Loss of epigenetic stability resulting in tumor heterogeneity has been recently described to frequently occur in cancer (14, 15). Studies of the CLL methylome have revealed an abundance of genes and other genomic regions that display altered DNA methylation states (16, 17), including methylation markers of high prognostic significance (18, 19). Despite the high frequency and importance of epigenetic alterations, the contribution of DNA methylation patterns to heterogeneity and evolution of tumor cell populations, and their relationship to genetic evolution, is currently undefined.

RESULTS

CLL Retains a Large Quantity of Allele-Specific Methylation

Global DNA methylation was evaluated in 68 CLL samples and 11 healthy donor B- and T-cell samples using Illumina human 450k BeadChip analysis. All samples were purified to >99% by CD19$^+$ or CD3$^+$ selection for B or T cells, respectively. To mitigate the influence of allele- and sample-specific variation in genomic sequence, all probes overlapping non unique sequences, single-nucleotide polymorphisms (SNP), and sample-specific copy-number alterations (CNA) were removed from all the 450k methylation profiles (see Methods). Although all CLL and healthy donor samples display an enrichment of CpG methylation values in the ranges of 0% to 20% (mainly CpG islands) and 80% to 100% (mainly gene body, intergenic CpGs, etc.) as observed previously (17), CLL samples display a distinct third peak of intermediate methylation values centered around 50% (Fig. 1A). The prominence of this peak is highly variable between CLL samples and it is not observed in healthy donor B- or T-cell samples. As diploidy is largely maintained in the genome of CLL cells (11), we hypothesized that the intermediate peak may be the result of allele-specific methylation (ASM). To test this possibility, we performed bisulfite sequencing (BS-seq) targeting differentially methylated regions (DMR) of imprinted gene clusters as well as non-imprinted regions where intermediately methylated (40%–60%) CpGs were identified. Twenty-eight amplicons were sequenced, including two imprinted domains as controls, in 20 CLL and four healthy donor B-cell samples with a median read depth of ~3,800 reads. Average CpG methylation determined by BS-seq was highly correlated with 450k β-values ($R^2 = 0.93$; Supplementary Fig. S1). Twenty-three amplicons contained sufficient SNP frequency to assign alleles.

All imprinted CpGs demonstrated a difference of >75% methylation between alleles; thus, this value was used for the definition of ASM in other amplicons (Fig. 1B). ASM can be readily observed in CLL samples. To determine the overall ASM composition of the intermediate peak on 450k profiles, 450k methylation values were plotted in comparison with the methylation difference between alleles in the 10 CLL samples most prominently displaying the intermediate peak (Fig. 1B). This comparison reveals that 85% of 450k values between 40% and 60% methylation (in non-imprinted regions) are monoallelically methylated in these samples, demonstrating that the bulk of the CLL-specific intermediate

peak results from ASM. Although healthy donor lymphocyte samples show values between 40% and 60%, only 0.4% of nonimprinted CpGs in healthy B cells exhibit ASM. Analysis of the patterns of CLL-specific ASM reveals that neighboring CpGs possess ASM on opposite alleles at random within individual amplicons (Supplementary Fig. S2). This is in contrast with the imprinted regions where methylation always occurs solely on the same allele (in both healthy and CLL cells), indicating that the majority of CLL-specific ASM does not signify imprinting. This complex pattern of stable allelic methylation has been suggested to likely occur via active demethylation (20). Moreover, this feature also suggests that ASM in CLL may be distinct from the large partially hypomethylated domains observed in other cancers (14, 21).

Genomic features associated with allele-specific CpG methylation (ASM-CpG) in CLL were analyzed by 450k arrays in the 10 CLL samples in which ASM was most prominently observed. On average, only 20% of the ASM-CpGs are found within CpG islands and 31% in the vicinity of gene transcriptional start sites, and thus are more similar in their genomic distribution to CpGs generally found to be fully methylated than those found to be unmethylated (Fig. 1C). Indeed, 78% of the CLL ASM-CpGs are fully methylated in the healthy donor B cells, suggesting that ASM in CLL mostly results from loss of methylation on one allele (Supplementary Fig. S3). This bias toward the allele-specific loss of methylation is consistent in comparisons with the other B-cell subtypes, including naïve CD5^{+} and memory-type B cells. Furthermore, ASM does not occur in patient-matched non-CLL leukocytes (Supplementary Fig. S4). In contrast to CpGs in low or high methylation ranges, the ASM state of individual CpGs shows a very low (2.7%) recurrence in CLL samples (Fig. 1C). Although the bulk of ASM seems to occur by chance, some ASM may recur nonrandomly between the samples (Supplementary Fig. S5). A Gene Ontology survey of all genes enriched for ASM (>25% of CpGs/gene equaling an average of ~10% of genes annotated per Gene Ontology group) revealed no significant enrichment of ontology terms. Of the 2.7% recurrent CpGs, 28% are located within known imprinted regions and 58% also display ASM in healthy B cells. After censoring these CpGs, only 0.4% of overall ASM in CLL is recurrent and potentially disease-specific.

The prevalence of ASM-CpGs in 450k profiles is highly variable between individual CLL samples (Fig. 1A and D). To estimate the levels of genome-wide ASM, the proportion of enriched intermediate CpG methylation values was determined by extrapolating a hypothetical curve connecting fully methylated and unmethylated distributions (see Methods; Fig. 1D). Using this method, we estimate that genomic monoallelic methylation ranges broadly from 2% to 10% of total CpGs in CLL (Fig. 1E). Healthy lymphocytes are estimated to possess <1% monoallelic methylation, consistent with other genome-wide assessments (22, 23). To validate and further explore ASM on a genome-wide level, ASM was assessed in whole-genome BS-seq (WGBS) data of two CLL samples and three healthy B-cell subtypes (17). The prevalence of ASM-CpGs was found to be approximately 6- to 8-fold higher in CLL samples relative to healthy B-cell subtypes (Supplementary Fig. S6). Furthermore, the number of ASM-CpGs determined by WGBS is closely proportional to the estimated amount by 450k analysis in the different CLL samples (Fig. 1E). In comparing 450k ASM estimations in other cancers (17, 24–27), CLL retains 3- to 5-fold more ASM (Fig. 1F). Together, these results suggest that ASM in CLL is first due to a monoallelic loss

of methylation before or during the establishment of the CLL founder clone, followed by high-fidelity maintenance methylation, which preserves methylation patterns *in cis* throughout subsequent generations of cells.

Methylation Heterogeneity in CLL

To investigate the basis for the high degree of variation in ASM between CLL samples, we hypothesized that the degree of ASM reflects intrasample heterogeneity of DNA methylation patterns. In a diploid cell, CpG methylation values are restricted to three states (methylated, unmethylated, and monoallelically methylated). If a population of cells maintains a stable, clonal pattern of methylation, values derived from a sample containing large numbers (usually $>1.0 \times 10^7$) of cells will also be restricted to these three discrete ranges of CpG methylation values. As all CpGs found within CNAs have been removed from the analysis, methylation values that occur between these discrete ranges can be caused only by a disparate CpG methylation state between cells within the sample. The total amount of CpGs that fall outside the expected ranges can thus be used to estimate the overall level of methylation heterogeneity in a given sample. This approach of elucidating intrasample heterogeneity has been used previously in conjunction with the HELP genome-wide methylation assay (28). Here, intrasample methylation heterogeneity is calculated by summing all values between 20% and 80% methylation subtracted by the amount of estimated genomic ASM (see Methods). Figure 2A displays the area of the 450k methylation value density plots used to define methylation heterogeneity in two CLL samples showing different levels of heterogeneity and in healthy donor B- and T-cell samples. Methylation heterogeneity values for all samples are displayed in Fig. 2B . Because of the polyclonal nature of healthy B- and T-cell populations, healthy donor lymphocyte samples would be anticipated to display methylation heterogeneity, as subtypes of B and T cells exhibit distinct, genome-wide patterns (17, 29). Indeed, healthy donor B- and T-cell samples display a relatively higher level of methylation heterogeneity. B cells extracted from lymph nodes display higher methylation heterogeneity levels compared with peripheral blood B cells, likely due to the high degree of B-cell diversification that occurs within germinal centers. Interestingly, methylation heterogeneity values in CLL are not normally distributed (Anderson–Darling test, $P < 0.001$), with a group of cases clustering below the median (12.5%) level of methylation heterogeneity. The non-normal distribution and median value is comparable with an additional CLL 450k dataset ($P < 0.001$; ref. 17). For this reason, this median methylation heterogeneity value is used to distinguish low and high methylation heterogeneity groups for subsequent analysis.

To confirm the accuracy of methylation heterogeneity estimations from 450k profiles, we used BS-seq to determine the intrasample heterogeneity of methylation patterns in CLL and healthy B-cell samples. For this, we used the calculation of epipolymorphism (EPM; ref. 15), which is a measurement of the observed consistency of a given pattern of methylation within a small defined region of neighboring CpGs (3–6 CpGs) versus the expected, random pattern. Low EPM values indicate that methylation patterns are similar between cells in a population, whereas elevated EPM values reflect higher heterogeneity. We calculated EPM from the BS-seq data generated on 20 CLL and four healthy donor B-cell samples. Healthy donor B-cell samples demonstrate a low degree of pattern consistency, with all possible

methylation states represented in proportions that would mostly be expected by chance (Fig. 2C). In contrast, most CLL samples demonstrate a higher degree of pattern consistency and, in some amplicons, only a single dominant pattern (epi-allele) per allele. These consistent methylation patterns are observed despite highly discordant methylation existing between neighboring CpGs and between alleles (see also Supplementary Fig. S2B). Correlation of intrasample methylation heterogeneity values with the average EPM across 25 amplicons reveals a general agreement between the two methods ($R^2 = 0.86$), although methylation heterogeneity evaluations by 450k slightly underestimates the high intrasample heterogeneity found by EPM in healthy donor samples (Fig. 2D).

Following confirmation of methylation heterogeneity estimations from 450k data, we first asked whether the level of genomic ASM is dependent on the amount of methylation heterogeneity in a given CLL sample. ASM and methylation heterogeneity exhibit a strong inverse correlation in CLL ($R^2 = 0.66$; Supplementary Fig. S7). By definition, the existence of ASM requires an allelic CpG methylation pattern to be highly consistent in a given population of cells (to fulfill the criteria of a 75% methylation difference between alleles). Therefore, it is intuitive that higher levels of overall methylation heterogeneity reflect lower levels of ASM, and indicates that variable methylation of ASM–CpG partially contributes to the overall level of methylation heterogeneity in a sample. Despite acute myleogenous leukemia (AML) and CLL possessing similar levels of methylation heterogeneity (Fig. 2B), AML exhibits a much lower level of ASM. This implies that ASM and methylation heterogeneity are not merely two measures of the same underlying phenomenon, and thus the high level of ASM in CLL is a distinctive feature of the disease. Analysis of solid tumor data yields consistently higher overall methylation heterogeneity levels in comparison with CLL and AML. As the estimation of methylation heterogeneity is highly influenced by sample purity, it is likely that the true levels of heterogeneity between tumor cells are overestimated in these samples. Absolute tumor cell content in solid cancers ranges from 30% to 90% (30); however, glioblastomas possess >90% tumor nuclei in most samples and display higher methylation heterogeneity than all CLLs investigated (Supplementary Fig. S7). Together, these results reveal that CLL exhibits a high level of genomic ASM relative to other leukemias and solid tumors, and that this distinctive feature is facilitated by—but is not specifically a result of—a low overall level of heterogeneity in the disease.

Next, we investigated whether methylation heterogeneity is associated with disease-related factors, such as prognostic indicators and patient outcome. First, we compared various disease markers of high prognostic significance, including *IGHV* mutation status (31), *ZAP70* methylation (19), and cytogenetic profiling (32). Patients with an unmutated *IGHV* gene, unmethylated *ZAP70*, and/or high-risk cytogenetics, including deletion of 11q and 17p, are generally associated with a more aggressive disease course. CLLs with above-median methylation heterogeneity are more frequently *IGHV* unmutated and have low *ZAP70* methylation (Table 1). Samples that were taken after therapy also are found to possess high methylation heterogeneity more frequently than samples from nontreated patients. However, it is problematic to attribute treatment as a direct cause of high methylation heterogeneity, as high methylation heterogeneity is associated with poor prognosis and thus a greater likelihood of treatment. Indeed, patients with untreated CLL

displaying an above-median methylation heterogeneity before therapy show a significantly reduced ($P = 0.006$) time from sampling to their first treatment (Fig. 2E). This suggests that epigenetic heterogeneity in the pretreatment window is associated with a more aggressive disease course.

The Relationship between Epigenetic and Genetic Heterogeneity

Next, we tested whether the methylation heterogeneity correlates with genetic heterogeneity in CLL samples. To assess genetic heterogeneity, we postulated that biologically significant subclonal populations would be identified by genomic events that have been shown to be relevant to CLL biology. Thus, we assessed in each CLL sample: (i) the total number and proportion of rearranged/mutated *IGHV* sequences by quantitative PCR (qPCR), Sanger, and next-generation sequencing approaches; (ii) the frequency of recurrent somatic mutations in the exons of *TP53*, *NOTCH1*, *SF3B1*, *MYD88*, *KRAS*, and *BRAF* by high-coverage 454-based sequencing; and (iii) the proportional copy number of large (>1 Mb) genomic aberrations by a nonbiased, genome-wide approach derived from 450k arrays (24) and by targeting recurrent CNAs in chromosomes 11, 13, and 17 using Taq-Man qPCR. Finally, FISH and karyotype data were also used to establish whether common CNAs were monoallelic or biallelic. Using these quantitative data, the clone size that each mutation and/or CNA represents was assigned in each sample. To designate a single value of genetic heterogeneity to each sample, we identified from all available genetic data the mutation and/or CNA clone size that would yield the most heterogeneous ratio of the two largest clones. This value is termed here as the genetic clone ratio. Using this approach, 66 of 68 CLL samples were assigned a genetic clone ratio (Supplementary Table S1). Figure 3A illustrates the determination of the genetic clone ratio in two CLL samples. We observe a strong relationship between methylation heterogeneity and genetic heterogeneity, with higher methylation heterogeneity values observed with increasingly heterogeneous genetic clone ratios (Fig. 3B; $P < 0.0001$). Samples scored as biclonal (more than one primary founder CLL population detected by *IGHV* rearrangements) were assessed separately and were found to have high levels of methylation heterogeneity. These data indicate that intrasample methylation heterogeneity is connected to the degree of genetic diversification and relative proportions of subclonal populations.

To further investigate the relationship between epigenetic and genetic heterogeneity, we focused on 28 CLL cases where samples were taken at two or more time points (median difference of 29 months; range, 12–113). The mutation and/or CNA clone size for each aberration per sample was determined. The degree of change between the time points for each case was defined by the mutation/CNA showing the greatest difference. Representative CLL cases showing <20% (no/low change) or >50% (large changes) in genetic clone ratios are displayed in Fig. 4A and B, respectively. The difference in overall methylation was measured by calculating the correlation between time points using the top 40k most variable probes between time points in all serial cases. CLL cases without genetic evolution demonstrate consistent methylation between time points, whereas cases that show high genetic evolution also show widespread methylation changes over time.

In total, 13 of 28 serial cases were observed to undergo a genetic change of >20% (Fig. 5A and B). By defining a difference between groups by both the number of CpGs that differ by >10% and the R^2 value (see Supplementary Fig. S8 for a detailed description of group dichotomization), 9 of 13 cases display evolution of methylation as defined by more than 5 $\times 10^3$ differentially methylated CpGs and $R^2 < 0.95$. The genetic aberrations that are observed to evolve codependently with methylation involve a subset of recurrent mutations and/ or CNAs. The majority of these aberrations (i.e., those involving *TP53, SF3B1, BRAF*, del11q23, del17p13, etc.) have been previously described as subclonal cancer driver mutations that are frequently associated with genetic evolution (11). Decrease or extinction of some mutations/CNAs is found to occur, indicating that a potential hierarchy of aberrations exists between subclonal populations. The four cases that do not show evolution of methylation, yet show a >20% change in genetic clone ratio, specifically involve changes detected solely at the 13q14 locus, hinting that some aberrations may not be linked to methylation evolution. Epigenetic and genetic changes are highly codependent (Fisher exact test, $P < 0.001$), as widespread epigenetic evolution independent of genetic evolution is not observed.

Prediction and Outcome of Methylation Evolution

We next investigated whether evolution of DNA methylation is associated with prognostic indicators or with specific genetic markers. Comparing the 9 serial cases that showed methylation evolution versus the 19 cases that showed no/low evolution, we find a significant enrichment of *IGHV*-unmutated and low *ZAP70*-methylated cases ($P = 0.002$; Table 2). Intriguingly, those cases that showed a high level of methylation heterogeneity in early sample time points predicted the occurrence of evolution ($P = 0.002$), supporting the notion that high methylation heterogeneity may result from active evolution. Methylation evolution is also associated with intervening treatment, as 8 of 9 evolving (vs. 7 of 19 nonevolving) cases received treatment between time points ($P = 0.01$); however, based on the finding that high methylation heterogeneity predicts a shorter time to treatment (Fig. 2E), it is likely that evolution provokes treatment in at least an equal manner to treatment inducing evolution. The only mutation or CNA that was significantly associated with predicting methylation evolution was *TP53* ($P = 0.03$), although the general low frequency of mutations in CLL necessitates a larger cohort of evolving cases for further testing. Overall, the presence of a subclonal mutation/CNA (<80% clone size) predicted methylation evolution ($P = 0.04$); whereas the presence of a clonal mutation did not, mirroring the findings of predicting genetic evolution (11).

Next, we tested the association between methylation evolution and the response to first-line therapy by comparing the presence of methylation evolution with the duration of the event-free time window following first-line therapy. Treatment and death were included as posttherapy events. All patients included were previously untreated upon first sampling and subsequently treated with purine analog and/ or alkylating therapy (Supplementary Table S1). Patients exhibiting methylation evolution experienced posttherapy events in a substantially shorter time than those lacking evolution (Fig. 5C; median = 9 vs. 110 months; $P = 0.0001$). Together, these observations demonstrate an association between methylation

evolution and poor prognostic and genetic indicators, as well as a lack of a durable response to therapy and a more aggressive disease course.

DISCUSSION

CLL generally exhibits a remarkable stability of DNA methylation. Combining the findings of others (12) with our findings, we demonstrated that CLL tumor populations maintain a precise overall pattern of DNA methylation for many years of disease course. Furthermore, as near-clonal patterns of methylation can be found in the cells of some patients, a perfect maintenance of methylation states must occur from the initial, founding epigenetic patterns associated with disease transformation. In these highly stable clones, the vast amount of CpG methylation that occurs only on one allele in nearly all cells is likely a simple reflection of the methylation status of the original founder clone. CLL arises in a relatively mature cell type that has some hallmarks of memory-type B cells, which may contribute to its stability phenotype compared with some other leukemias. It is tempting to draw a parallel between the general indolent nature of the disease and the extreme stability of the epigenome in some patients. Here, we also show that in contrast to the high stability of DNA methylation generally observed in the disease, a subset of cases demonstrate elevated levels of methylation heterogeneity. Above-median levels of methylation heterogeneity are associated with poor prognostic indications, a shorter time to treatment, and greater subclonal genetic diversification.

The association of *IGHV* mutation status and other prognostic markers with our findings advocates the integration of DNA methylation heterogeneity and evolution, along with associated genetic aberrations, into the established high/ low-risk subtype model of CLL (Fig. 6). In this integrated view, ASM occurs in the founder malignant cell as a result of monoallelic loss of methylation associated with B-cell maturation (17) and/or transforming events. Establishment is also usually associated with the acquisition of recurrent CLL founder mutation(s), such as trisomy 12, *MYD88*, and others (11). Highly stable, clonal CLLs, which are much less likely to coevolve epigenetic and genetic changes, are typically the *IGHV*-mutated/*ZAP70*-methylated subtype. These cases generally exhibit low methylation heterogeneity and require less immediate treatment. Evolution of methylation is not observed to occur in the absence of newly acquired and actively selecting genetic aberrations. In a minority of cases, a genetic change can be detected without an appreciable change in methylation. In these cases, the observed change in 4 of 4 patients is solely a change at the 13q14 locus, a common aberration in the low-risk CLL subtype. CLL cases with above-median methylation heterogeneity, including all of those that display methylation evolution, are associated with *IGHV*-unmutated/*ZAP70*-unmethylated markers. In this high-risk disease subtype, increasing methylation heterogeneity is associated with an increasingly complex subclonal genetic architecture. In all cases that show methylation evolution, a change in genetic architecture is observed. Evolving genetic aberrations in this subset of cases involve known cancer driver genes, including *TP53*, *SF3B1*, *BRAF*, etc.

How does coevolution of epigenetics and genetics occur? There are two main (non–mutually exclusive) hypotheses (Fig. 6). In the first, *simultaneous acquisition*, a novel mutation of a cancer driver gene is acquired in a cell that fundamentally alters the biology of the cell in a

way that involves changes to the epigenome. The second, *stepwise acquisition*, involves a mechanism in which first there exists a low level of epigenetic instability producing variation within the CLL population. When a cell from this population then acquires a novel cancer driver mutation, the variant methylation pattern of the particular cell hitchhikes on the subsequent subclonal expansion. This expansion then permits the detection of the altered methylation pattern that would otherwise be detectible only on a single-cell level previous to the expansion.

Why are epigenetic and genetic changes associated? A possibility one must first consider is that they are mechanistically unrelated. In the stepwise acquisition scenario, it is possible that epigenetic drift occurs independently of the stochastic acquisition of driver mutations. Another possibility is that they are mechanistically linked. Associated genetic and epigenomic states have been observed in several other cancers, including mutations in *IDH1/2* in gliomas (33) and myeloid malignancies (34), *H3F3A* in glioblastomas (24), and *BRAF* in colorectal cancer (35). In most of these well-described associations, mutations occur in genes with defined roles in epigenetic pathways (reviewed in ref. 4). However, a direct causative connection to epigenetic regulation remains elusive. It stands to reason that many recurrent, high-impact mutations, not known to directly involve epigenetic regulation, also involve epigenetic deregulation as a part of their aberrant function. For example, the deletion of chromosome 17p is associated with a loss of methylation at repetitive sequences in CLL (36). The most judicious scenario places genetic events as the driving force behind the subsequent evolution of a novel epigenetic state. However, one cannot exclude that primary changes to the epigenome permit the acquisition of specific mutations, that is, epigenetic silencing of key tumor-suppressors that would otherwise have resulted in apoptotic cell death/senescence (37). Epigenetic drift may endow a subset of cells within the population with the eventual attributes needed to escape negative feedback regulation by tumor suppressors, allowing for a driver mutation to occur. Here, we observe that epigenetic/genetic coevolution involves a spectrum of aberrations, implying a potentially very broad and intricate interrelationship between the genome and epigenome. Using higher-resolution techniques, future work will involve unraveling the relative contributions of epigenetic versus genetic evolution to disease, and investigate whether monitoring DNA methylation heterogeneity during disease course will benefit patients.

METHODS

CLL and Healthy Donor Lymphocyte Samples

Clinical and biologic characteristics of the 107 samples of patients with CLL and healthy donor controls used for DNA methylation analysis are shown in Supplementary Table S1. CLL cases were selected to provide a balanced cohort for *IGHV* mutation status (28 of 68; <98% identity), treatment status (19 of 68 untreated, 19 of 68 treated after sampling, 30 of 68 treated before sampling), and treatment response to first-line therapy (28 complete/partial response, 13 stable/progressive disease). Furthermore, samples were enriched for the presence of informative somatic aberrations. Thus, the cohort is not a true representation of the general CLL population at large. FISH, *IGHV* mutation, and *ZAP70* methylation analysis was done as previously described (19, 32, 38). All patients gave informed consent.

Isolation and Purification of CLL and Healthy Lymphocytes

All samples were obtained from whole blood, subjected to Ficoll-Isopaque density centrifugation, and CD19+ B and CD3+ T cells were isolated by positive magnetic cell separation (Miltenyi Biotec). Sorted cells were checked for purity by fluorescence-activated cell sorting (FACS) with CD19/CD20 for healthy control samples and CD19/ CD20/CD5 for CLL samples (BD Biosciences). Following sorting, all samples with a CD19/CD20/CD5 purity <98% were subjected to additional sorting, and the average final purity of all sorted samples was >99%. CLL samples with >100 × 10^6 WBC/μL were not subject to purification. DNA was extracted from purified cells using the Qiagen DNeasy Kit (Qiagen) and quantified using a ND-100 spectrophotometer (Thermo Scientific).

DNA Methylation Analysis Using 450k BeadChip Arrays

High-quality genomic DNA (500 ng) was bisulfite converted using the EZ DNA Methylation Gold Kit (Zymo Research). The Infinium methylation assay was carried out as described previously (39). Data from the 450k Human Methylation Array were normalized by the Beta Mixture Quantile (BMIQ) method (40) using the RnBeads analysis software package (41). Data are available at the European Genome–Phenome Archive (EGAS00001000534). GenomeStudio (Illumina, Inc.) was used for CpG island and gene segment annotation; repetitive sequence, segmental duplication, SNP, and imprinted DMR annotation was obtained from the UCSC genome browser, version hg19. Estimation of genomic ASM from 450k methylation frequency plots was calculated by first generating a hypothetical third-degree polynomial curve that estimates the distribution without intermediate methylation values (i.e., from unmethylated and fully methylated distributions) with smooth connections at fixed departure points (matching the original function at these departure points in the first derivative). Estimated ASM is the quantity of methylation values above the hypothetical curve and below the actual density curve relative to all values analyzed (multiplied by 100 for scaling purposes). Methylation heterogeneity was calculated by measuring the quantity of methylation values below the hypothetical curve and between 20% and 80% methylation (again multiplied by 100). This methylation window represents the range in which the greatest difference occurs between clonal CLL and healthy lymphocyte (polyclonal) samples. Different variable and fixed methylation heterogeneity window settings were tested and did not significantly change the relative order of methylation heterogeneity sample values or the association of methylation heterogeneity versus outcome (Supplementary Fig. S9). The reproducibility of estimated genomic ASM and methylation heterogeneity values was confirmed by testing two independent samples in two CLL cases; each sample was independently isolated and purified (Supplementary Fig. S10). Because each CLL sample may have a unique CNA profile, in addition to censoring all probes on chromosome arms 11q, 13q, 17p, and 12p+q in all 450k profiles, any CNA >1 Mb in size was censored in sample-specific manner. Censoring was matched between serial samples. CNAs were detected using an algorithm for quantitative CNA detection based on 450k probe intensities (24). CLL 450k profiles were also censored for all nonunique sequences, probes possibly containing SNPs, and sex chromosomes (totaling ~185K CpGs). Additional CLL and healthy B-cell 450k/WGBS data, presented in Figs. 1, 2, and Supplementary Figs. S3, S6, and S7, were obtained from previously published work (17),

AML (25), glioblastoma (24, 26), renal clear cell carcinoma (26), colon adenocarcinoma (27), and lung adenocarcinoma (26).

Analysis of ASM Using WGBS

WGBS data were obtained from the International Cancer Genome Consortium (http://icgc.org). ASM–CpG were determined by identifying heterozygous SNPs using the Bis–SNP algorithm (42) followed by determining the allelic methylation ratio of each CpG within overlapping reads (minimum 8 reads per allele). The calculation of the ASM to investigated CpG ratio required the ASM–CpG to have a *P* value smaller than FDR 0.05 and a methylation difference of at least 75%. CpGs were only considered if not overlapping an SNP. All CpGs were filtered that are located in problematic regions (HISEQDEPTH, REPEAT_MASKER, DUKE_EXCLUDED, and DAC_BLACKLIST tracks obtained from the UCSC Genome Browser, hg19).

Targeted BS-seq and Analysis

Bisulfite-converted genomic DNA was amplified by standard PCR using barcoded primers for patient sample identification. Primer sequences, SNPs, and 450k probes covered are listed in Supplementary Table S2. Multiple PCR products from 12×2 samples were pooled and sequenced using paired-end, 150-bp reads on a MiSeq sequencer (Illumina, Inc.). Median read depth per amplicon per patient was ~3,800 high-quality reads. Debarcoded reads were analyzed simultaneously for methylation and genotype using the Bis–SNP algorithm (42). EPM analysis was performed as previously described (15) with modifications. To normalize EPM values derived from amplicons with different numbers of CpGs and variable average methylation content, expected EPM values were first generated by random simulation of methylation patterns for amplicons containing three to six CpGs for average methylation ranges of 20% to 80%. Spline curves derived from simulations were used to adjust EPM for average methylation content of each amplicon in each sample using: $EPM = EPM_{observed} + (1 - EPM_{expected})$. Amplicons with an average methylation <20% or >80% were excluded from EPM analysis due to low complexity potential.

Identification of Genomic Aberrations and Determination of Genetic Heterogeneity in CLL Samples

Somatic genetic aberrations were assessed in 106 CLL samples. For each sample, the sequence identity of the unique rearranged *IGHV* region was determined by genescan qPCR followed by Sanger dye-terminator sequencing (38). Biclonality was defined by a CLL sample exhibiting a minimum of three unique and fully recombined *IGHV* alleles, with a minimum of two productive rearrangements. For samples with polyclonal chromatogram profiles, PCR products were sequenced using MiSeq to determine the sequence and proportion of subclones. The frequency of recurrent somatic SNVs in the exons of *TP53*, *NOTCH1*, *SF3B1*, *MYD88*, *KRAS*, and *BRAF* was determined by 454-sequencing (ref. 43; Roche). At least one mutation could be detected in 66 of 96 samples. All mutations were considered to be heterozygous. The proportional copy number of large (>1 Mb) CNAs was determined by a custom quantitative algorithm derived from 450k array raw data (24). The proportional copy number of recurrent minimally deleted regions (MDR) in chromosomes

11, 13, and 17 was further supported using TaqMan qPCR. Eight primer-probes were used to amplify various regions within each MDR and compared with eight primer-probes positioned at various genomic positions not affected by CNAs in all samples. CNAs could be detected in 88 of 96 samples. FISH data on chromosomes 6, 8, 11, 12, 13, 14, and 17 were used to establish whether common CNVs were monoallelic or biallelic. In all, quantitative SNV/CNA data could be determined for 93 of 96 samples.

Statistical Analysis

Associations between methylation heterogeneity, genetic heterogeneity, and clinical features were assessed by the Wilcoxon rank-sum test, Fisher exact test, or the Kruskal–Wallis test, as appropriate. Correlation calculations were performed by Pearson product-moment correlation coefficient (R^2). To test the significance of recurrence of ASM between samples we constructed a test statistic which is the number of ASM–CpGs occurring in at least 8 of 10 samples, then an empirical P value was calculated on the basis of 10,000 permutations. Time-to-event data were estimated by Kaplan–Meier analyses, and differences between groups were assessed using the Mantel–Cox log-rank test.

Supplementary Material

Refer to Web version on PubMed Central for supplementary material.

Acknowledgments

REFERENCES

1. Baylin SB, Jones PA. A decade of exploring the cancer epigenome— biological and translational implications. Nat Rev Cancer. 2011; 11:726–734. [PubMed: 21941284]

2. Broske AM, Vockentanz L, Kharazi S, Huska MR, Mancini E, Scheller M, et al. DNA methylation protects hematopoietic stem cell multipo-tency from myeloerythroid restriction. Nat Genet. 2009; 41:1207–1215. [PubMed: 19801979]

3. Trowbridge JJ, Snow JW, Kim J, Orkin SH. DNA methyltransferase 1 is essential for and uniquely regulates hematopoietic stem and progenitor cells. Cell Stem Cell. 2009; 5:442–449. [PubMed: 19796624]

4. Timp W, Feinberg AP. Cancer as a dysregulated epigenome allowing cellular growth advantage at the expense of the host. Nat Rev Cancer. 2013; 13:497–510. [PubMed: 23760024]

5. Gerlinger M, Rowan AJ, Horswell S, Larkin J, Endesfelder D, Gronroos E, et al. Intratumor heterogeneity and branched evolution revealed by multiregion sequencing. N Engl J Med. 2012; 366:883–892. [PubMed: 22397650]

6. Nik-Zainal S, Van Loo P, Wedge DC, Alexandrov LB, Greenman CD, Lau KW, et al. The life history of 21 breast cancers. Cell. 2012; 149:994–1007. [PubMed: 22608083]

7. Navin N, Kendall J, Troge J, Andrews P, Rodgers L, McIndoo J, et al. Tumour evolution inferred by single-cell sequencing. Nature. 2011; 472:90–94. [PubMed: 21399628]

8. Mullighan CG, Phillips LA, Su X, Ma J, Miller CB, Shurtleff SA, et al. Genomic analysis of the clonal origins of relapsed acute lymphoblas-tic leukemia. Science. 2008; 322:1377–1380. [PubMed: 19039135]

9. Ding L, Ley TJ, Larson DE, Miller CA, Koboldt DC, Welch JS, et al. Clonal evolution in relapsed acute myeloid leukaemia revealed by whole-genome sequencing. Nature. 2012; 481:506–510. [PubMed: 22237025]

10. Schuh A, Becq J, Humphray S, Alexa A, Burns A, Clifford R, et al. Monitoring chronic lymphocytic leukemia progression by whole genome sequencing reveals heterogeneous clonal evolution patterns. Blood. 2012; 120:4191–4196. [PubMed: 22915640]

11. Landau DA, Carter SL, Stojanov P, McKenna A, Stevenson K, Lawrence MS, et al. Evolution and impact of subclonal mutations in chronic lymphocytic leukemia. Cell. 2013; 152:714–726. [PubMed: 23415222]

12. Cahill N, Bergh AC, Kanduri M, Goransson-Kultima H, Mansouri L, Isaksson A, et al. 450K–array analysis of chronic lymphocytic leukemia cells reveals global DNA methylation to be relatively stable over time and similar in resting and proliferative compartments. Leukemia. 2013; 27:150–158. [PubMed: 22922567]

13. Stilgenbauer S, Sander S, Bullinger L, Benner A, Leupolt E, Winkler D, et al. Clonal evolution in chronic lymphocytic leukemia: acquisition of high-risk genomic aberrations associated with unmutated VH, resistance to therapy, and short survival. Haematologica. 2007; 92:1242–1245. [PubMed: 17666364]

14. Hansen KD, Timp W, Bravo HC, Sabunciyan S, Langmead B, McDonald OG, et al. Increased methylation variation in epigenetic domains across cancer types. Nat Genet. 2011; 43:768–775. [PubMed: 21706001]

15. Landan G, Cohen NM, Mukamel Z, Bar A, Molchadsky A, Brosh R, et al. Epigenetic polymorphism and the stochastic formation of differentially methylated regions in normal and cancerous tissues. Nat Genet. 2012; 44:1207–1214. [PubMed: 23064413]

16. Rush LJ, Raval A, Funchain P, Johnson AJ, Smith L, Lucas DM, et al. Epigenetic profiling in chronic lymphocytic leukemia reveals novel methylation targets. Cancer Res. 2004; 64:2424–2433. [PubMed: 15059895]

17. Kulis M, Heath S, Bibikova M, Queiros AC, Navarro A, Clot G, et al. Epigenomic analysis detects widespread gene-body DNA hypomethylation in chronic lymphocytic leukemia. Nat Genet. 2012; 44:1236–1242. [PubMed: 23064414]

18. Kanduri M, Cahill N, Goransson H, Enström C, Isaksson A, Rosen-quist R. Differential genome-wide array-based methylation pro-files in prognostic subsets of chronic lymphocytic leukemia. Blood. 2010; 115:296–305. [PubMed: 19897574]

19. Claus R, Lucas DM, Stilgenbauer S, Ruppert AS, Yu LB, Zucknick M, et al. Quantitative DNA methylation analysis identifies a single CpG dinucleotide important for ZAP-70 expression and predictive of prognosis in chronic lymphocytic leukemia. J Clin Oncol. 2012; 30:2483–2491. [PubMed: 22564988]

20. Ehrlich M, Lacey M. DNA hypomethylation and hemimethylation in cancer. Adv Exp Med Biol. 2013; 754:31–56. [PubMed: 22956495]

21. Hon GC, Hawkins RD, Caballero OL, Lo C, Lister R, Pelizzola M, et al. Global DNA hypomethylation coupled to repressive chromatin domain formation and gene silencing in breast cancer. Genome Res. 2012; 22:246–258. [PubMed: 22156296]

22. Fang F, Hodges E, Molaro A, Dean M, Hannon GJ, Smith AD. Genomic landscape of human allele-specific DNA methylation. Proc Natl Acad Sci U S A. 2012; 109:7332–7337. [PubMed: 22523239]

23. Xie W, Barr CL, Kim A, Yue F, Lee AY, Eubanks J, et al. Base-resolution analyses of sequence and parent-of-origin dependent DNA methylation in the mouse genome. Cell. 2012; 148:816–831. [PubMed: 22341451]

24. Sturm D, Witt H, Hovestadt V, Khuong-Quang DA, Jones DTW, Konermann C, et al. Hotspot mutations in H3F3A and IDH1 define distinct epigenetic and biological subgroups of glioblastoma. Cancer Cell. 2012; 22:425–437. [PubMed: 23079654]

25. Network CGAR. Genomic and epigenomic landscapes of adult *de novo* acute myeloid leukemia. N Engl J Med. 2013; 368:2059–2074. [PubMed: 23634996]

26. TCGA. [Accessed February 1, 2013] The Cancer Genome Atlas Data Portal. 2013. Available from: https://tcga-data.nci.nih.gov/tcga/tcgaHome2.jsp

27. Muzny DM, Bainbridge MN, Chang K, Dinh HH, Drummond JA, Fowler G, et al. Comprehensive molecular characterization of human colon and rectal cancer. Nature. 2012; 487:330–337. [PubMed: 22810696]

28. De S, Shaknovich R, Riester M, Elemento O, Geng HM, Kormaks-son M, et al. Aberration in DNA methylation in B-cell lymphomas has a complex origin and increases with disease severity. PLoS Genet. 2013; 9:e1003137. [PubMed: 23326238]

29. Ji H, Ehrlich LIR, Seita J, Murakami P, Doi A, Lindau P, et al. Comprehensive methylome map of lineage commitment from haematopoietic progenitors. Nature. 2010; 467:338–342. [PubMed: 20720541]

30. Carter SL, Cibulskis K, Helman E, McKenna A, Shen H, Zack T, et al. Absolute quantification of somatic DNA alterations in human cancer. Nat Biotechnol. 2012; 30:413–421. [PubMed: 22544022]

31. Hamblin TJ, Davis Z, Gardiner A, Oscier DG, Stevenson FK. Unmutated Ig V-H genes are associated with a more aggressive form of chronic lymphocytic leukemia. Blood. 1999; 94:1848–1854. [PubMed: 10477713]

32. Dohner H, Stilgenbauer S, Benner A, Leupolt E, Krober A, Bullinger L, et al. Genomic aberrations and survival in chronic lymphocytic leukemia. New Engl J Med. 2000; 343:1910–1916. [PubMed: 11136261]

33. Yan H, Parsons DW, Jin GL, McLendon R, Rasheed BA, Yuan WS, et al. IDH1 and IDH2 mutations in gliomas. N Engl J Med. 2009; 360:765–773. [PubMed: 19228619]

34. Mardis ER, Ding L, Dooling DJ, Larson DE, McLellan MD, Chen K, et al. Recurring mutations found by sequencing an acute myeloid leukemia genome. N Engl J Med. 2009; 361:1058–1066. [PubMed: 19657110]

35. Weisenberger DJ, D Siegmund K, Campan M, Young J, Long TI, Faasse MA, et al. CpG island methylator phenotype underlies sporadic microsatellite instability and is tightly associated with BRAF mutation in colorectal cancer. Nat Genet. 2006; 38:787–793. [PubMed: 16804544]

36. Fabris S, Bollati V, Agnelli L, Morabito F, Motta V, Cutrona G, et al. Biological and clinical relevance of quantitative global methylation of repetitive DNA sequences in chronic lymphocytic leukemia. Epigenetics. 2011; 6:188–194. [PubMed: 20930513]

37. Hinoue T, Weisenberger DJ, Pan F, Campan M, Kim M, Young J, et al. Analysis of the association between CIMP and BRAF(V600E) in colorectal cancer by DNA methylation profiling. PLoS ONE. 2009; 4:e8357. [PubMed: 20027224]

38. Kröber A, Seiler T, Benner A, Bullinger L, Brückle E, Lichter P, et al. V(H) mutation status, CD38 expression level, genomic aberrations, and survival in chronic lymphocytic leukemia. Blood. 2002; 100:1410–1416. [PubMed: 12149225]

39. Bibikova M, Le J, Barnes B, Saedinia-Melnyk S, Zhou LX, Shen R, et al. Genome-wide DNA methylation profiling using Infinium (R) assay. Epigenomics. 2009; 1:177–200. [PubMed: 22122642]

40. Teschendorff AE, Marabita F, Lechner M, Bartlett T, Tegner J, Gomez-Cabrero D, et al. A beta-mixture quantile normalization method for correcting probe design bias in Illumina Infinium 450 k DNA methylation data. Bioinformatics. 2013; 29:189–196. [PubMed: 23175756]

41. Assenov, Y.; Muller, F.; Lutsik, P.; Walter, J.; Lengauer, T.; Bock, C. [Accessed February 1, 2013] Comprehensive analysis of DNA methylation data with RnBeads. 2013. Available from: http://rnbeads.mpi-inf.mpg.de

42. Liu YP, Siegmund KD, Laird PW, Berman BP. Bis-SNP: combined DNA methylation and SNP calling for Bisulfite-seq data. Genome Biol. 2012; 13:R61. [PubMed: 22784381]

43. Hullein J, Jethwa A, Stolz T, Blume C, Sellner L, Sill M, et al. Next-generation sequencing of cancer consensus genes in lymphoma. Leuk Lymphoma. 2013; 54:1831–1835. [PubMed: 23621802]

44. Edelmann J, Holzmann K, Miller F, Winkler D, Buhler A, Zenz T, et al. High-resolution genomic profiling of chronic lymphocytic leukemia reveals new recurrent genomic alterations. Blood. 2012; 120:4783–4794. [PubMed: 23047824]

SIGNIFICANCE

Epigenetic alterations are pervasive in cancer and continually develop during disease progression; however, the mechanisms that promote changes in the tumor epigenome at large are currently undefined. The current work provides insight into the coevolution of genetic and epigenetic aberrations and highlights the influential role of genetic aberrations in the selection of novel methylation patterns.
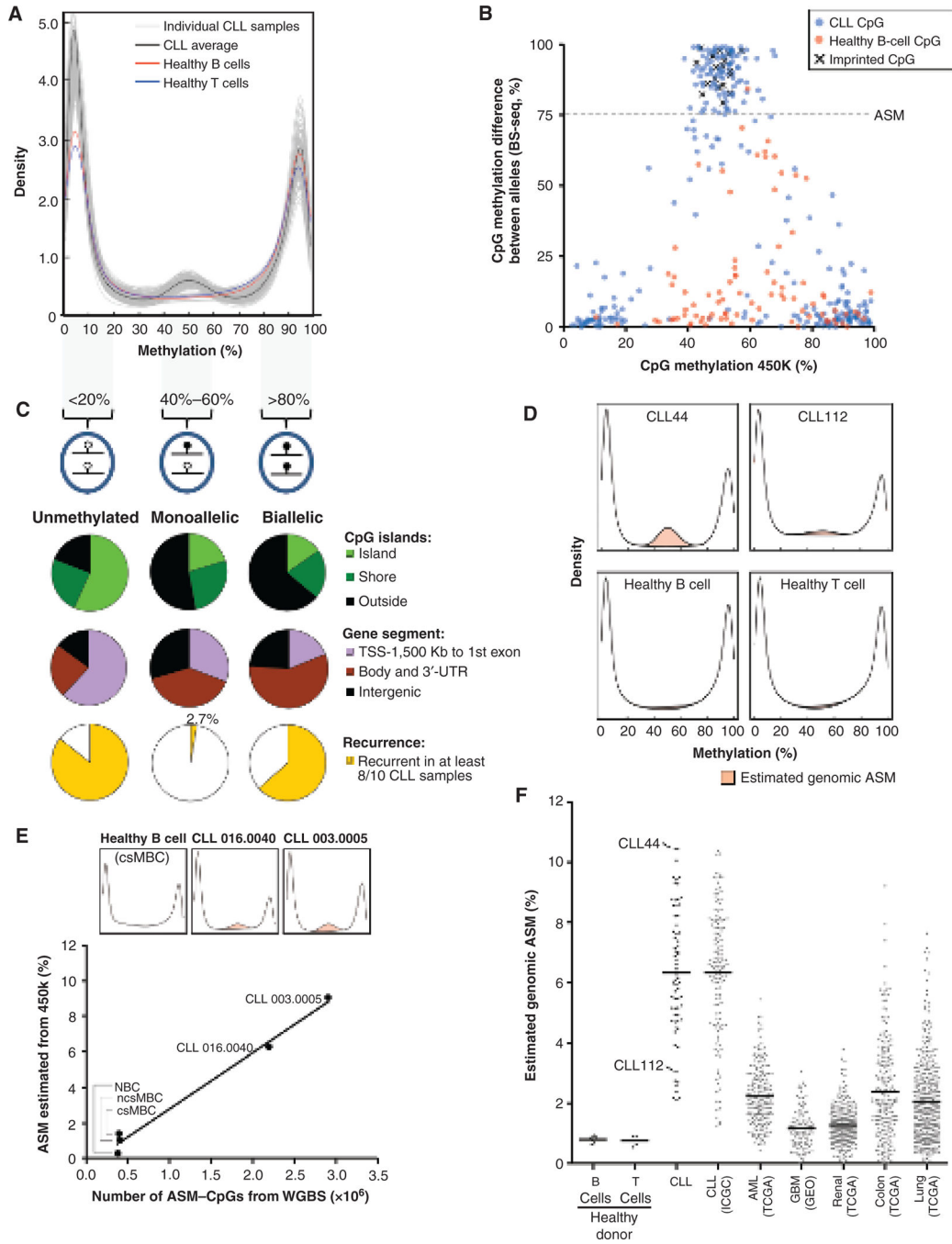
Figure 1.

Pronounced ASM in CLL samples. **A**, frequency distribution of CpG methylation values from 450k profiles in CLL and healthy donor B- and T-cell samples. CLL displays a prominent enrichment of methylation values centered around 50%. **B**, a scatterplot comparing 450k methylation versus the percentage methylation difference between alleles determined by BS-seq. CpGs from nonimprinted loci in CLL samples (blue dots), healthy B cells (red dots), and imprinted loci (black Xs) are shown. The range of methylation difference defined as allele-specific (>75% difference) is shown. **C**, genomic characteristics

of CpGs separated into unmethylated (0%–20%), monoallelic (40%–60%), and biallelically (80%–100%) methylated CpGs in clonal CLL samples. The proportion of CpGs associated with CpG islands, gene segments, and recurrence within each methylation range is displayed. **D**, methylation density plots of two CLL samples representative of high (CLL44) and low (CLL112) monoallelic methylation, as well as a healthy donor B- and T-cell samples, with the area used to estimate the overall proportion of genomic ASM highlighted. **E**, a comparison of ASM in WGBS with the estimation by 450k. 450k methylation density plots of one healthy B-cell sample and two CLL samples analyzed by 450k are shown (top) along with the correlation between methods. NBC, naïve B cell; ncsMBC, non-class-switched memory B cell. **F**, estimated ASM in all 68 CLL and healthy donor lymphocyte samples. Individual values for CLL samples illustrated in **D** are indicated. Analysis of downloaded 450k datasets (in gray) is included for comparison. CLL (17); AML (25); GBM, glioblastoma multiforme (24); Renal, renal clear cell carcinoma (26); Colon, colon adenocarcinoma (27); and Lung, lung adenocarcinoma (26). ICGC, International Cancer Genome Consortium; TCGA, The Cancer Genome Atlas.
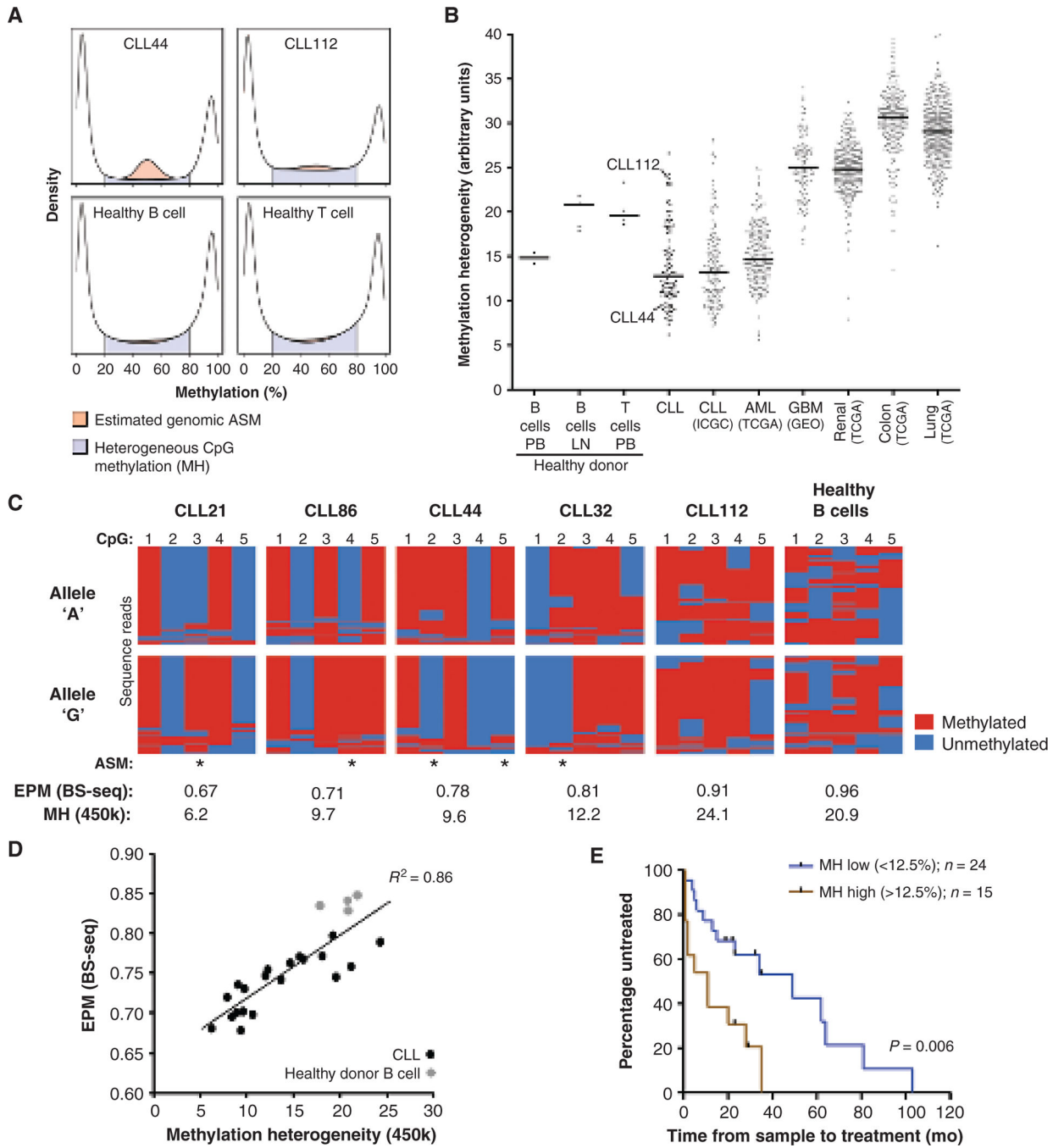
Figure 2.
Variable intratumor heterogeneity of DNA methylation heterogeneity in CLL samples. **A**, the proportion of 450k methylation values used to estimate the overall level of DNA methylation heterogeneity in representative CLL and healthy donor samples. **B**, methylation heterogeneity values show pronounced variation among CLL cases and collectively display lower methylation heterogeneity than healthy donor samples as well as other solid tumors. LN, lymph node; PB, peripheral blood. **C**, a representative example of targeted allele-specific bisulfite-sequencing (surrounding the SNP rs365605) showing mostly clonal

(CLL21, 44 and 86) and increasingly heterogeneous (CLL32, 112) methylation patterns among CLL samples. Despite disordered methylation states between neighboring CpGs (horizontal), many CLL samples display mostly clonal patterns indicated by a high proportion of identical epi-alleles (vertical). Epipolymorphism (EPM) and overall 450k methylation heterogeneity values are displayed; asterisks indicate ASM-CpGs. **D**, correlation between methylation heterogeneity and the average EPM for 25 targeted regions in 20 CLL and four healthy donor B-cell samples demonstrates an agreement between the two methods. **E**, the duration of treatment-free survival from the time of sampling to first therapy. CLL samples were segregated into two groups by the median methylation heterogeneity value of all samples.
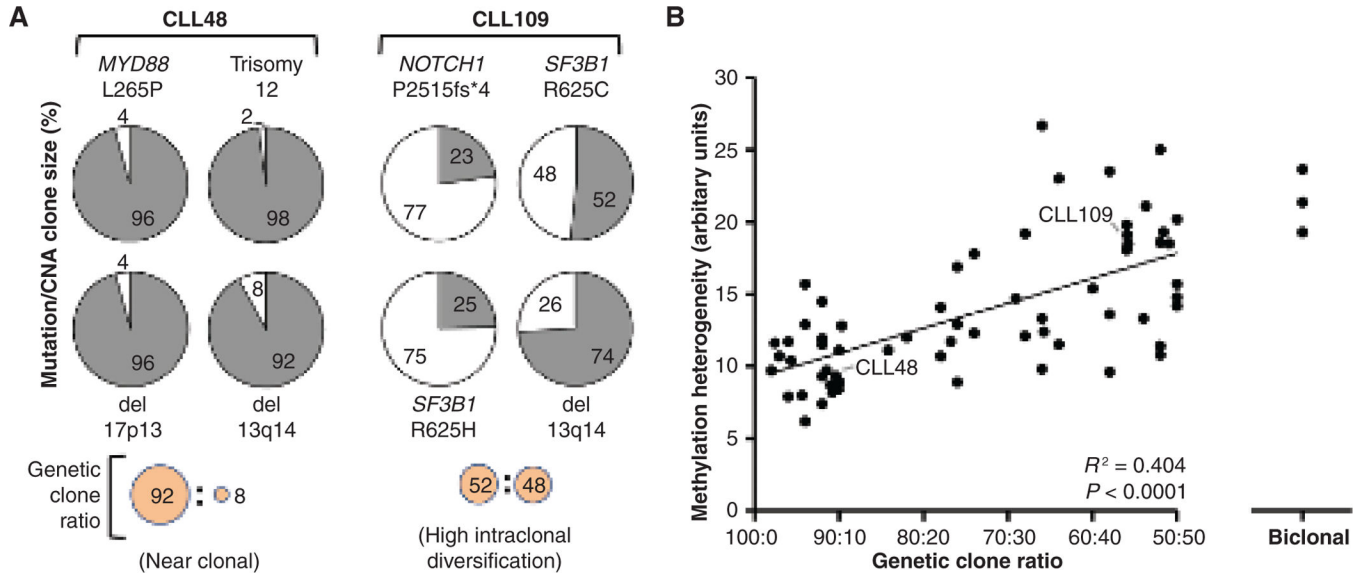
Figure 3.
Epigenetic heterogeneity is associated with genetic heterogeneity in CLL samples. **A**, quantitative assessment of the mutation/CNA clone sizes for various aberrations in two CLL samples representative of different levels of genetic heterogeneity. Clone sizes for various detected somatic aberrations (gray) are displayed for CLL48 and CLL109. For CLL48, all variations fall within a range consistent with a clonal sample population possessing monoallelic aberrations at 13q14, 17p13, and *MYD88* and a single-copy gain of chromosome 12. For CLL109, individual somatic variations occur at a frequency indicative of intraclonal diversification, with the mutation clone size of the R625C mutation in *SF3B1* representing approximately an even ratio of genetic clones. The most possible heterogeneous ratio of all mutations/CNAs is designated as the genetic clone ratio for a given sample. **B**, methylation heterogeneity levels of all CLL samples versus the genetic clone ratio. Biclonal samples are also displayed.
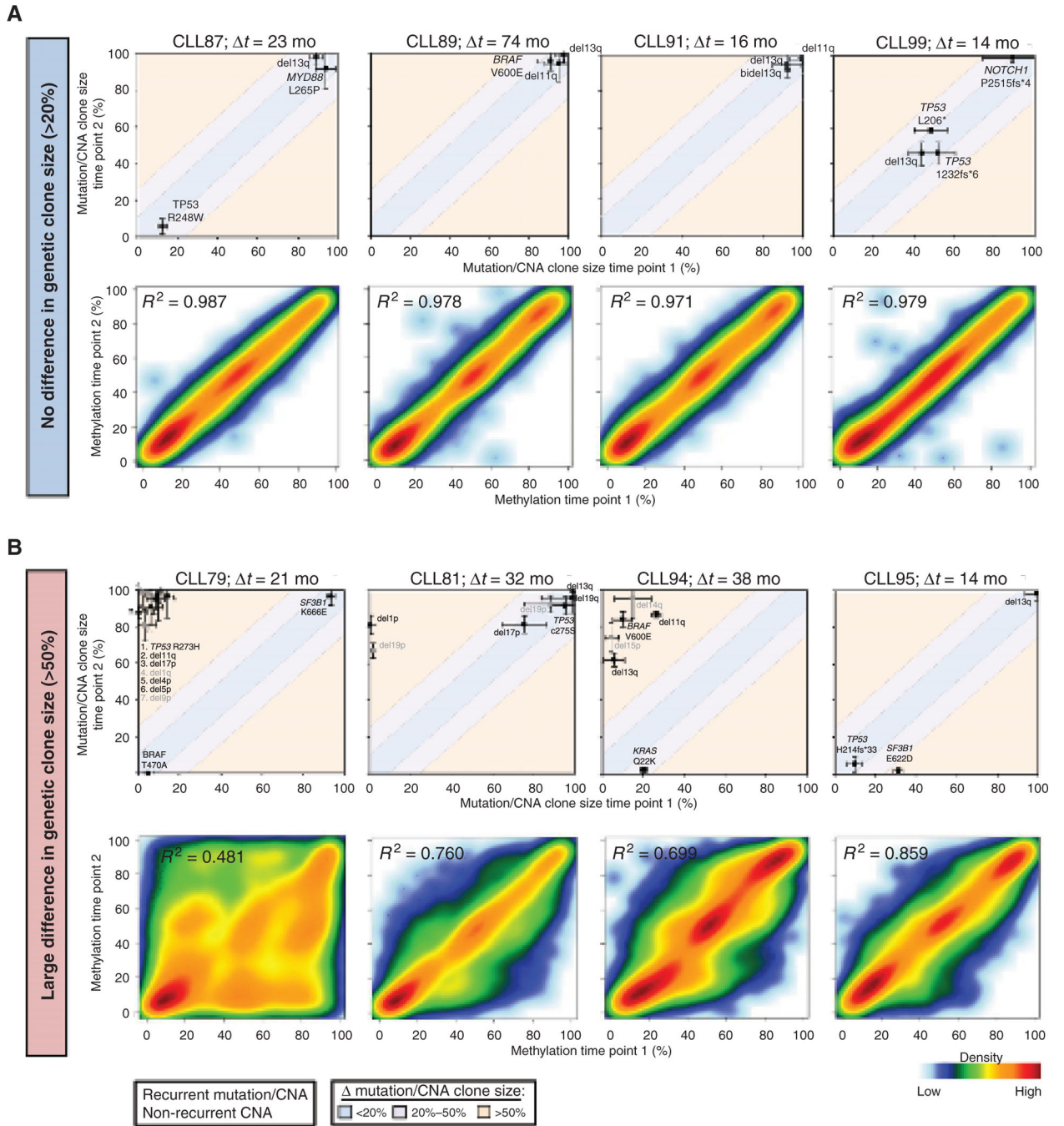
Figure 4.
Coordinated epigenetic and genetic evolution in 28 serial CLL cases. **A**, representative CLL cases showing no/low change (<20%) and (**B**) large change (>50%) in genetic clone size are displayed. The time elapsed between sampling is displayed above each panel. The mutation/CNA clone size determined for each aberration is shown for both time points (above); error bars indicate SD of technical replicates. Recurrent CLL aberrations, defined by Edelmann and colleagues (44), are labeled in black, nonrecurrent CNAs in gray. Differences in clone size between time points that would represent a change of <20%, 20%–

50%, and >50% are illustrated by light blue, purple, and pink areas, respectively. For each sample, the methylation values of the overall 40k most variable CpGs are used to calculate the Pearson correlation coefficient (R^2) between time points.

A

Number of differentially methylated CpGs (×10³)

- No/low change
- Coevolution
- Genetic change only (Δ13q14)

$R^2 = 0.85$

Change in genetic clone ratio (%)

B

Summary table of evolving mutations/CNAs in serial CLL cases:

CLL case	Change in methylation (R^2)	Number of ΔCpGs (×10³)	% Change in genetic clone ratio	Change in mutation/CNA clone size (%)
CLL79	0.481	33.3	100	TP53(83), 13q14*(100), many CNAs†(90–100)
CLL94	0.699	19.2	74	BRAF(74), KRAS*(18), 11q23(62)
CLL81	0.760	16.3	70	1p, 19p(70)
CLL95	0.859	12.5	29	SF3B1*(29)
CLL36	0.874	12.2	32	TP53(32), 17p13(16), 6p(19)
CLL63	0.865	12.2	36	11q23(36)
CLL84	0.889	10.1	30	13q31-33(30)
CLL93	0.915	9.1	46	IGHV(46), BRAF(25)
CLL80	0.937	8.9	34	TP53(34), SF3B1(24)
CLL86	0.960	5.5	30	13q14*(30)
CLL90	0.953	4.8	32	13q14(32)
CLL62	0.971	3.9	24	13q14(24)
CLL88	0.983	1.5	24	13q14(24)
15x cases	0.977 ± 0.01	2.3 ± 1.4	0.05 ± 0.02	No alteration detected > 20%

*Extinction/decrease of mutation or CNA-bearing population
†See Fig. 4 and Supplementary Table 1 for full list of CNAs

C

% Event-free following first therapy

DNA methylation:
- No/low evolution; n = 13
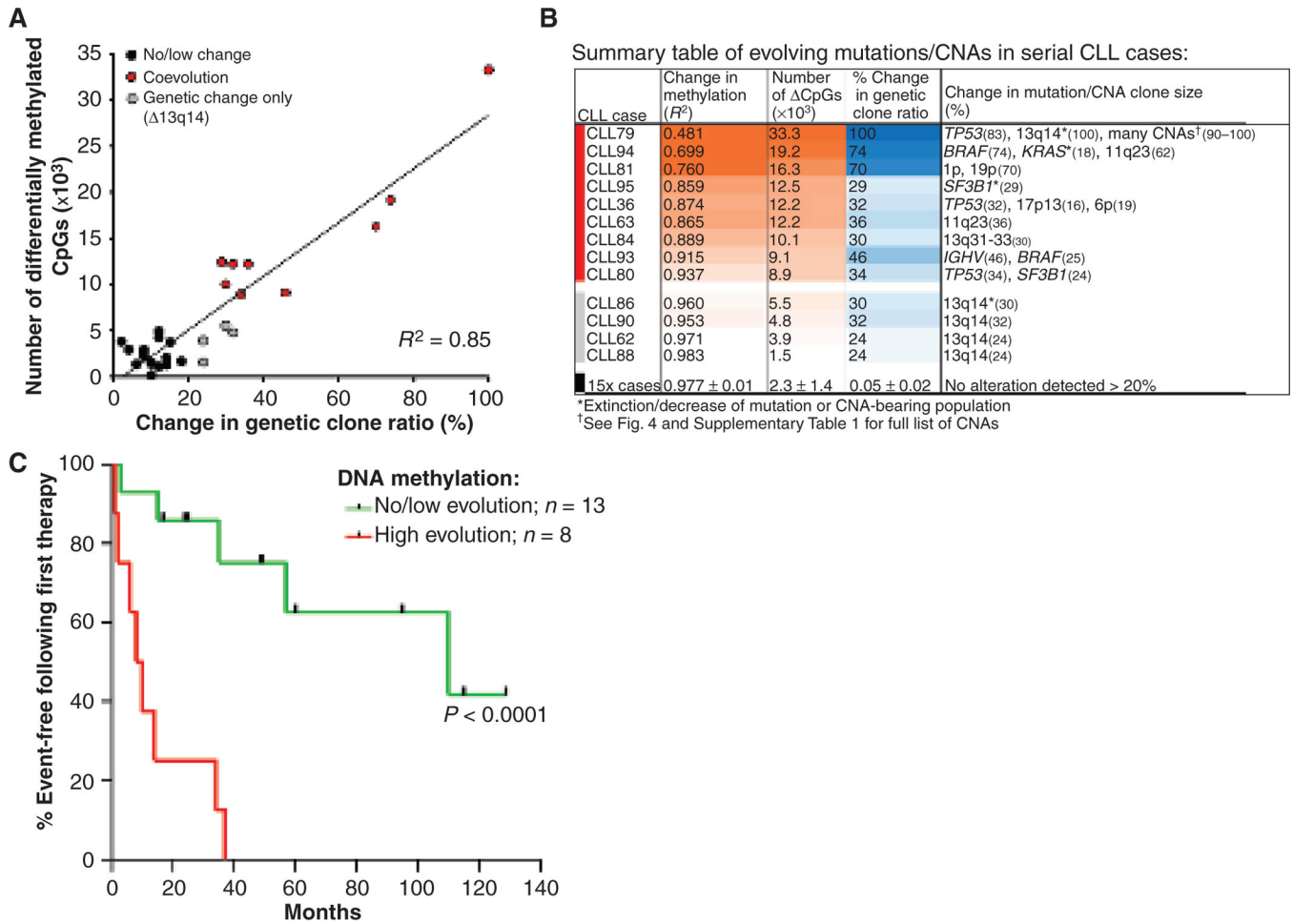- High evolution; n = 8

$P < 0.0001$

Months

Figure 5.

Evolution of DNA methylation versus genetic aberrations and event-free survival following first therapy. **A**, correlation of genetic evolution (measured by the change in the genetic clone ratio) with methylation evolution (measured by the number of differentially methylated CpGs >10%) in 28 serial CLL cases. Cases that show no/low methylation or genetic evolution (black dots) and coevolving cases (red dots) are shown. Cases that show only genetic evolution are colored gray. **B**, a summary of methylation and genetic evolution in serial cases. The change in methylation (measured by the number of differentially methylated CpGs and the Pearson correlation) and the change in the genetic clone ratio, including the evolving genetic aberrations, are shown for each case. **C**, a comparison of the duration of the event-free time window following first-line therapy between CLL cases with high and no/low methylation evolution. Second treatment or death were used as posttherapy events. Statistical analysis performed by Mantel-Cox log-rank test (*P*< 0.0001).
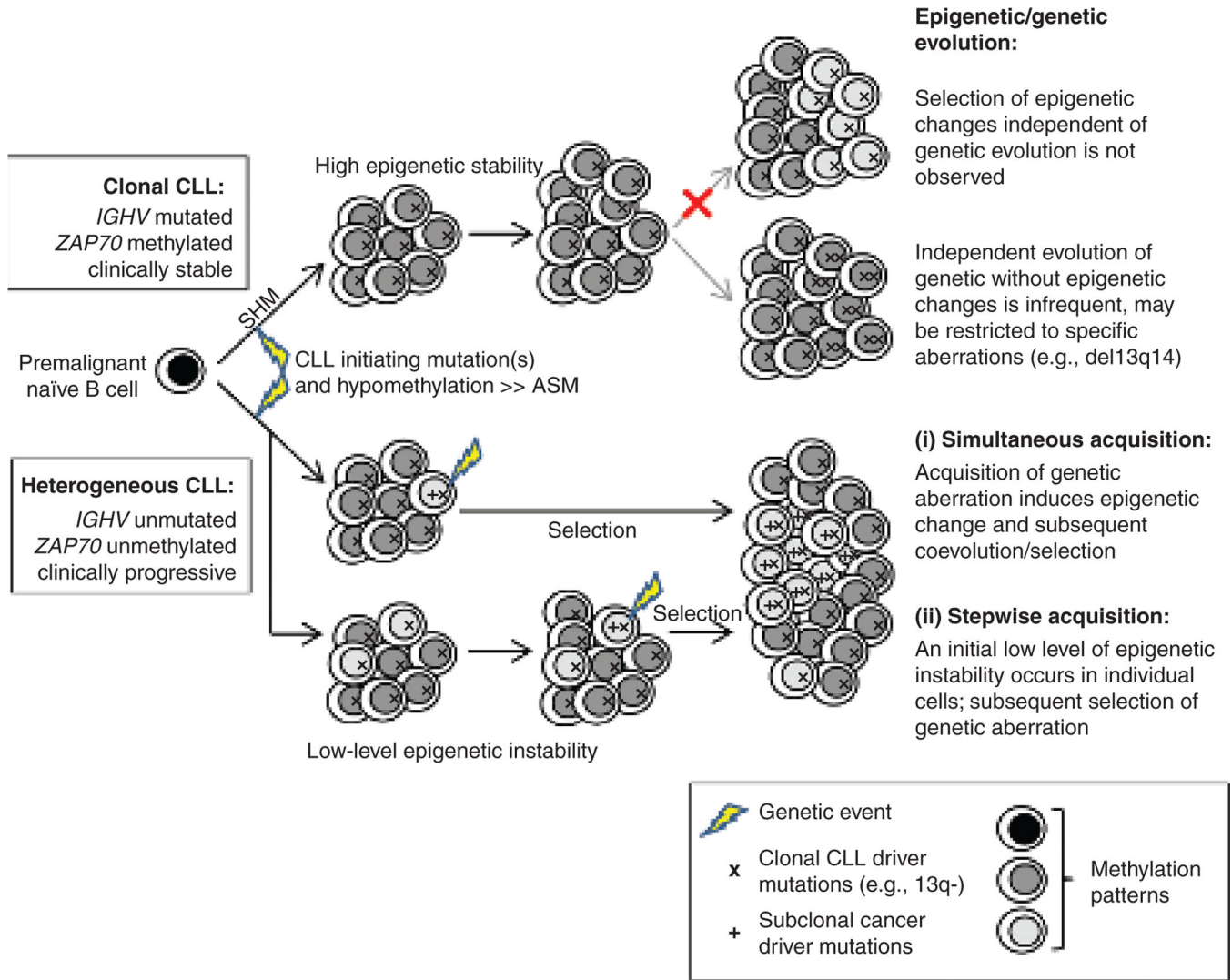
Figure 6.

Scenarios involving epigenetic and genetic evolution in the two-disease subtype model of CLL. CLL-initiating events include genome-wide hypomethylation, which produces a high degree of ASM, and usually a somatic genetic event, which together are observed as clonal aberrations at all time points. In the *IGHV* -mutated subtype, the genome-wide DNA methylation pattern of the founder cell is maintained with relative high fidelity. Selection of subclonal populations with widespread epigenetic changes is not observed. Genetic evolution independent of methylation evolution is only rarely observed and frequently involves a recurrent deletion that includes 13q14. All cases that exhibit a high degree of methylation evolution are the *IGHV*-unmutated disease subtype and involve simultaneous selection of genetic aberrations. Two possible (non-mutually exclusive) hypotheses for coincident evolution are shown: (i) simultaneous acquisition, where the acquisition of a genetic subclonal driver aberration directly affects the epigenetic state of the subclonal founder cell, and (ii) stepwise acquisition, where a low level of epigenetic stability precedes

the acquisition of a genetic subclonal driver, and thus a novel epigenetic pattern is coselected with the genetic aberration. SHM, somatic hypermutation.

Table 1

Comparison of methylation heterogeneity with patient characteristics and prognostic indicators

	Low DNA methylation heterogeneity no. (%)	High DNA methylation heterogeneity no. (%)	*P*
Patient characteristics			
Age at diagnosis (y ± SD)	55.8 ± 11.8	59.9 ± 10.6	n.s.
Sex (female)	10 (33)	15 (48)	n.s.
Pretreatment (yes)	6 (19)	13 (42)	**0.014**
Prognostic indicators			
IGHV unmutated	8 (35)	11 (79)	**<0.01**
ZAP70 low methylation	7 (30)	9 (69)	**0.024**
Cytogenetics (NK, sole −13q)	14 (61)	9 (69)	n.s.

Abbreviation: n.s., not significant.

Table 2

Summary table of prognostic and genetic markers in serial CLL cases (time point 1)

	No/low evolution of DNA methylation *n* = 19 (%)	High evolution of DNA methylation *n* = 9 (%)	*P*
Prognostic indicators			
IGHV unmutated	7 (37)	9 (100)	**0.002**
ZAP70 low methylation	7 (37)	9 (100)	**0.002**
High methylation heterogeneity	5 (26)	8 (89)	**0.002**
Cytogenetics			
Normal karyotype	4 (21)	2 (22)	n.s.
Del 13q14	12 (63)	6 (67)	n.s.
Del 11q23	4 (21)	1 (11)	n.s.
Del 17p13	3 (16)	1 (11)	n.s.
Del 6q	1 (5)	1 (11)	n.s.
Trisomy 12	3 (16)	1 (11)	n.s.
Genetic mutations			
TP53	**3 (16)**	**5 (56)**	**0.03**
SF3B1	4 (21)	3 (33)	n.s.
NOTCH	3 (16)	0	n.s.
MYD88	3 (16)	0	n.s.
BRAF	1 (5)	2 (22)	n.s.
KRAS	0	1 (11)	n.s.
Mutation clone size			
Clonal (>80%)	7 (37)	1 (11)	n.s.
Subclonal (<80%)	**5 (26)**	**6 (67)**	**0.04**
Any	11 (58)	7 (78)	n.s.